Clean synthetic strategies to dopamine-based biologically active molecules from lignin: A green path to drug discovery

Authors: Anastasiia M. Afanasenko[1], Xianyuan Wu[1§], Alessandra De Santi[1§], Walid A. M. Elgaher[2], Andreas M. Kany[2], Roya Shafiei[2,3], Marie-Sophie Schulze[4], Thomas Schulz[4], Jörg Haupenthal[2], Anna K. H. Hirsch[2,3*], Katalin Barta[1,5]*

Affiliations:

[1]Stratingh Institute for Chemistry, University of Groningen; Nijenborgh 4, 9747 AG Groningen, the Netherlands.

[2]Helmholtz Institute for Pharmaceutical Research Saarland (HIPS) − Helmholtz Centre for Infection Research (HZI); Campus Building E8.1, 66123 Saarbrücken, Germany.

[3]Department of Pharmacy, Saarland University; Campus Building E8.1, 66123 Saarbrücken, Germany.

[4]Institute of Virology, Hannover Medical School, 30625 Hannover, Germany

[5]Institute for Chemistry, University of Graz; Heinrichstrasse 28/II, 8010 Graz, Austria.

[§]Equal contribution

*Corresponding author. E-mail: katalin.barta@uni-graz.at, anna.hirsch@helmholtz-hips.de

Abstract: The structural complexity of renewable resources offers remarkable opportunities for the environmentally friendly manufacturing of essential pharmaceuticals, yet this has not been adequately addressed due to the lack of suitable methods. Our here described approach to drug discovery, builds on the innate structural features of the aromatic moiety of lignin to enable green pathways to various classes of biologically active molecules of the core dopamine structure. The catalytic transformations are atom-economic, produce only harmless side-products and use benign reaction media, including tunable deep eutectic solvents for modulating reactivity in challenging cyclization steps. Biological screening and chemical similarity searches identified promising anti-infective, anti-inflammatory, and anticancer activities. The frontrunners show outstanding metabolic stability and *in vivo* activity against *Streptococcus pneumoniae* infection, highlighting the power of our strategy.

One-Sentence Summary: The inherent structural features of lignin inspire green methods for the synthesis of diverse biologically active compound classes and future drug candidates.

Main Text: Active pharmaceutical agents are essential for human well-being, and represent a large and continuously growing market (*1*, *2*). However, pharmaceutical manufacturing frequently relies on classical synthesis methods, which require the use of hazardous chemicals and toxic, volatile organic solvents and result in copious amounts of chemical waste (*3*). The use of renewable starting materials in the earliest stages of drug design offers excellent opportunities for the integration of the main principles of Green Chemistry into the manufacturing practices of pharmaceuticals – a top priority in this sector (*4–7*). While making complex molecules from petrochemicals requires multi step syntheses that ultimately lead to high E factors (*3*); renewable resources and derived platform chemicals bear sufficient structural diversity to be – in principle – transformed into sophisticated scaffolds with great synthetic efficiency and high atom-economy (*8*, *9*). Moreover, biomass resources currently considered for the development of sustainable biorefinery schemes already incorporate structural moieties often found in naturally occurring biologically active compounds (*10*, *11*). Surprisingly the immense benefit of developing such sustainable strategies has not been fully recognized, since viable pathways to 'connect' renewable raw material streams with suitable biologically active compound classes, and lead target molecules, have not been adequately explored (*4*, *6*, *12*).

Lignin, the largest renewable source of aromatics on the planet, has attracted significant attention to the sustainable production of fuels, materials and chemicals (*13–15*), with lesser attention devoted to fine chemicals (*16–18*). Here we present an array of waste-minimized chemo-catalytic strategies, that allow unprecedented access to numerous classes of biologically active molecules, by matching lignin depolymerization with appropriate clean functionalization protocols. This strategy connects our unique lignin derived platform chemical (4-((1,3-dioxolan-2-yl)methyl)-2-methoxyphenol), **C2-G-EG-acetal** to pharmaceutically relevant molecules and natural products based on the dopamine platform, in just a few efficient catalytic steps, relying chiefly on hydrogen borrowing methodologies (*19*, *20*), and the use of tunable deep eutectic solvents (DES) (*21*) for challenging cyclization steps.

Systematic experimental screening of the obtained compound libraries for anti-infective and anti-cancer activities was followed by in-depth evaluation of the most promising hits. This led to the identification of compound **5ff** that showed a promising *in vitro* ADME profile and emerged as frontrunner against the Gram-positive pathogen *Streptococcus pneumoniae*, one of the World Health's Organisation's global priority pathogens; this was also confirmed in an *in vivo* infection model with *Galleria mellonella* larvae. Moreover, subjecting the compound libraries to a chemical similarity search using FDA-approved drugs predicted potential biological activities, such as anti-herpesvirus and anti-inflammatory activities, which were successfully validated against Kaposi's sarcoma-associated herpesvirus (KSHV) and cyclooxygenase-2 as a molecular target, respectively.

The promising biological activities, combined with the efficient and modular synthetic routes developed, demonstrates an example of rapid discovery of active scaffolds for the development of pharmaceuticals from renewable resources.

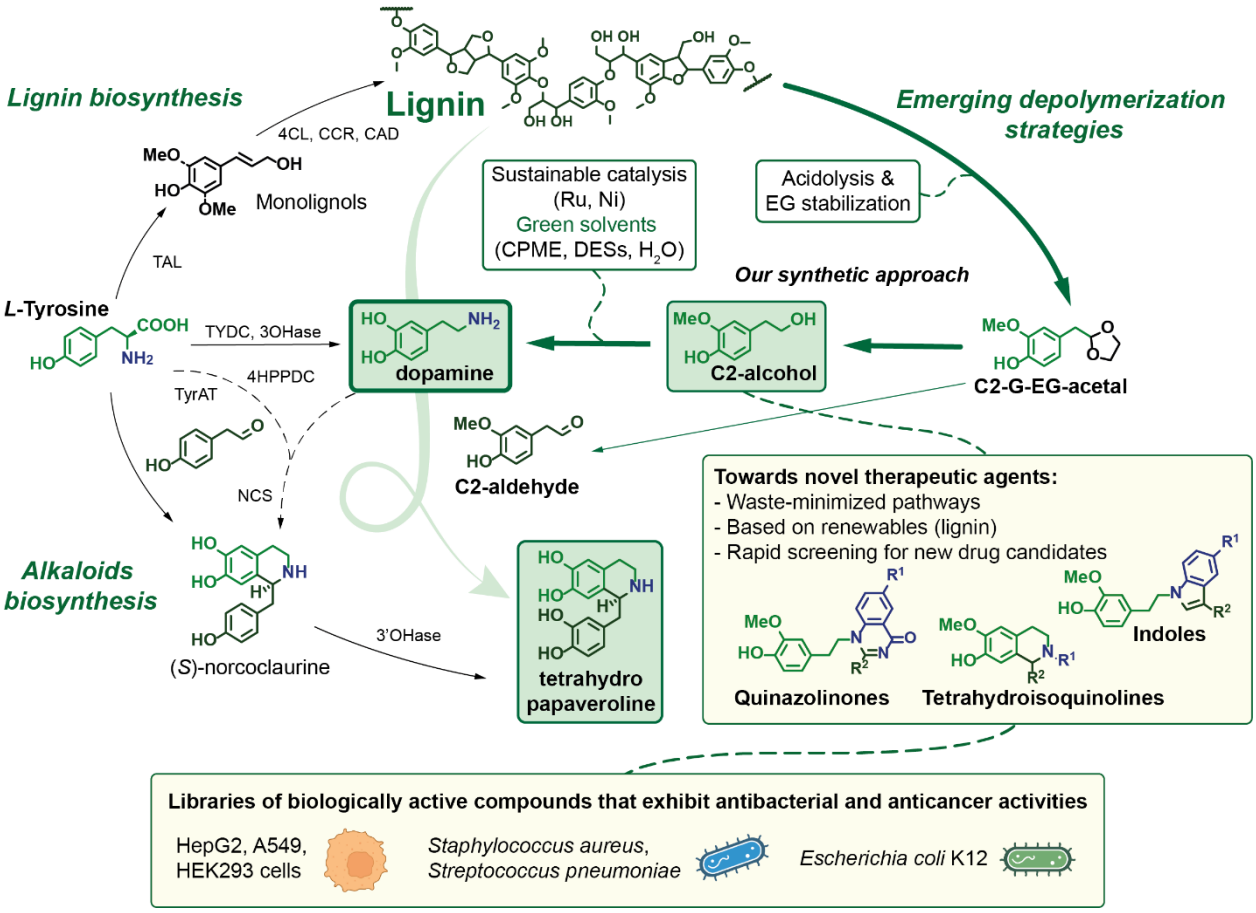

Figure 1. Green paths toward novel therapeutic agents and the natural product tetrahydropapaveroline, starting from *L*-Tyrosine (natural approach - left) *vs.* lignin-derived monomer C2-G-EG-acetal (right). Abbreviations of the enzymes: TYDC – tyrosine decarboxylase, TyrAT – tyrosine aminotransferase, 4HPPDC – 4-hydroxyphenylpyruvate decarboxylase, NCS – norcoclaurine synthase, 3OHase – tyramine 3-hydroxylase, 3′OHase – norcoclaurine 3-hydroxylase, TAL – tyrosine ammonia-lyase, 4CL – 4-coumarate: CoA ligase, CCR – cinnamoyl-CoA reductase, CAD – cinnamyl alcohol dehydrogenase.

The foundation of our approach is the acidolysis and ethylene glycol stabilization method pioneered in our laboratory, which leads to **C2-G-EG-acetal** in high selectivity and near theoretical yield from lignin or even lignocellulose (*22–24*). Interestingly, while most cutting-edge 'lignin-first' methods result in ethyl-, propyl- or propanol- aromatics (*25*), our unique acidolysis/stabilization approach directly leads to the C2-aldehyde platform, owing to the dominance of the deformylation/C–O scission pathway through acidolysis of the β-O-4 moiety, under the conditions applied (*26*, *27*).

Direct conversion of C2-G-EG-acetal to homovanillyl alcohol (HA)

First, we have explored the direct conversion of the **C2-G-EG-acetal** into its stable C2-alcohol analogue, homovanillyl alcohol (**HA**). The desired **C2-G-EG-acetal** deprotection/C=O hydrogenation sequence was examined using various heterogeneous hydrogenation catalysts, assuming a reductive approach (**Table S1**). While low to moderate **HA** yields (27–63%) were seen with Ru/C, Ru/Al_2O_3, Pd/C using *tert*-amyl alcohol as a solvent, excellent conversion and **HA** selectivity was achieved in water, presumably due to a more favorable acetal-to-aldehyde deprotection step. Particularly, employing Ru/Al_2O_3 resulted in a 98% yield at 140 °C and with 20 bar hydrogen (**Table S1**, entry 5). Further optimizing the reaction conditions (5% Ru/Al_2O_3, 20 bar H_2, 90 °C, 4.5 h), **HA** was obtained in a 92% isolated yield (**Table S1**, entry 9).

Next, we developed suitable hydrogen borrowing methodologies (*8*, *16*, *19*) for the direct catalytic amination of **HA** with ammonia or primary amines. Thereby **HA** serves as central

platform to provide rapid and waste-minimized access to dopamine (**Scheme 1**) or libraries of secondary amines (**Figure 2** and **3**), precursors to more complex molecules.

Natural product synthesis from lignin – tetrahydropapaveroline

Benzylisoquinoline alkaloids (BIAs) possess diverse pharmacological properties, including the analgesics codeine and morphine, the antimicrobial agents sanguinarine and berberine, the muscle relaxant (+)-tubocurarine, and the antitumor drug noscapine (*28–30*). Despite the remarkable structural diversity, BIAs share a common biosynthetic pathway (*31*, *32*) starting with the key branch-point intermediate (*S*)-norcoclaurine, resulting from the condensation and subsequent cyclization of the two tyrosine-derived compounds **dopamine**, which forms the core isoquinoline scaffold and 4-hydroxyphenylacetaldehyde (**4-HPAA**) that occupies the C1-linked position (**Figure 1**, on the left). Interestingly, Nature skillfully utilizes *L*-tyrosine for the production of both **dopamine** and **4-HPAA** through a variety of biocatalytic cascades, involving *ortho*-hydroxylation and then decarboxylation, and deamination followed by decarboxylation, correspondingly (*32*).

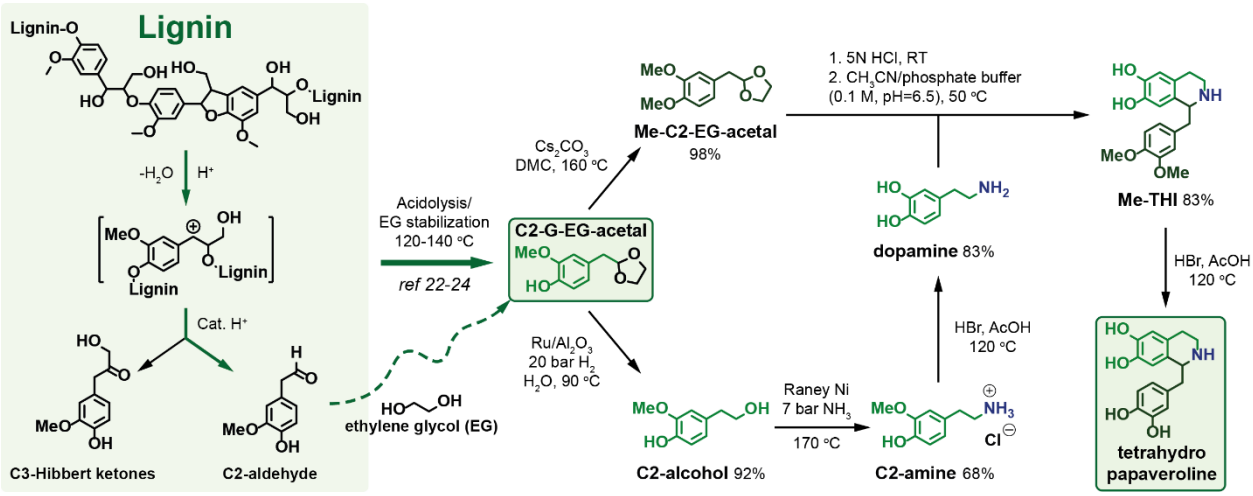

Scheme 1. Overall scheme for the synthesis of natural product tetrahydropapaveroline starting from lignocellulose or lignin *via* the aromatic platform chemical – C2-G-EG-acetal.
Catalytic method for obtaining **C2-G-EG Acetal** in high selectivity is acidolysis in conjunction with EG stabilization, whereby softwood lignin (*22*, *23*) or lignocellulose (*24*) might be used as starting material under indicated conditions.

Interestingly, our newly designed chemo-catalytic strategy that starts from softwood lignin, follows a conceptually different pathway, yet leads to a similar product outcome: the formation of 1-(3,4-dimethoxybenzyl)-1,2,3,4-tetrahydroisoquinoline-6,7-diol (**Me-THI**) (**Scheme 1,** see also Supplementary Information, Section 9). Herein, the **C2-G-EG-acetal** obtained *via* lignin acidolysis/EG stabilization serves as the core building block for accessing *both coupling partners*, namely **dopamine**, *via* the challenging direct catalytic amination of **HA** by ammonia, and the C2-aldehyde source upon *in situ* C2-acetal deprotection. Following these considerations, the synthetic strategy for constructing the natural product tetrahydropapaveroline from lignin is detailed in **Scheme 1**. Hereby, we accomplished the challenging direct coupling of **HA** with ammonia in the presence of Raney-Ni to deliver **C2-amine**, followed by demethylation to afford the target **dopamine**, in 83% isolated yield, without the need for additional purification procedures. This constitutes a straightforward catalytic sequence from softwood lignocellulose (*24*) or softwood lignin (*22*, *23*, *33*) to **dopamine**, an essential medicine, widely used in the treatment of Parkinson's disease (*34*). The subsequent formation of the core tetrahydroisoquinoline scaffold (**Me-THI**) was realized through the coupling between **dopamine** and **Me-C2-aldehyde** generated *in situ* from the corresponding

Me-C2-EG-acetal, which was in turn obtained by methylation of the parent lignin platform chemical **C2-G-EG-acetal**, using the green methylation agent dimethyl carbonate (DMC). The critical Pictet–Spengler cyclization and the **Me-C2-EG-acetal** deprotection steps required the same mild, acidic reaction conditions, allowing for the development of a one-pot procedure. Finally, cleavage of the methyl ethers in **Me-THI** by hydrobromic acid afforded the target **tetrahydropapaveroline** in 89% yield. The developed sequence allows for an overall 6.24 wt% yield of dopamine and 5.65 wt% yield of the natural product **tetrahydropapaveroline**, showing excellent efficiencies (46.2% and 34.1%, respectively), calculated on lignin basis.

Catalytic conversion of HA to aminoalkyl-guaiacol derivatives

Having an efficient method at our disposal for the production of **HA** from **C2-G-EG-acetal**, we created a library of dopamine derivatives in order to access new pharmaceutically-relevant structures. Thus, we have developed the direct catalytic amination of **HA** with a range of aniline derivatives, applying the homogeneous Ru-based Shvo's catalyst (**C1**), thereby building on our previous experiences in the selective catalytic amination of lignocellulose-derived dihydroconiferyl and dihydrosinapyl alcohols (*8*). To find optimum reaction conditions, we have studied the catalytic coupling of **HA** with aniline, in the presence of **C1** (**Table S2**). Interestingly, the **C2-alcohol** (**HA**) turned out to be more reactive than its C3-analogues, affording the target secondary amine **3a** in perfect selectivity (99%) and good isolated yield (74%), using the non-toxic solvent CPME and 0.5 mol% **C1** without any additives at 120 ^{o}C (**Table S2**, entry 6). Further expanding the scope of this Ru-catalyzed amination methodology resulted in a library of aminoalkyl-guaiacols (**Figure 2A**) comprising existing structures with already identified, as well as new structures with potential therapeutic applications. For example, the secondary amines **3b′** and **3k′** are precursors in the synthesis of orexin receptor antagonists (*35*), which are used to treat sleep disorders, as well as isoalloxazine derivatives (*36*), agents for treatment of Alzheimer's disease. Potentially, **3q′** can serve as a key building block for the synthesis of erythrina alkaloids (*37*, *38*), that possess sedative, hypotensive, and CNS activities. In addition, **3q** could be used as a building block for the synthesis of bio-based polymers (*39*). In our hands, the synthetized aminoalkyl-guaiacols have shown various biological activities, as shown on the **Figure 2A** and summarized in Supplementary Information in Section 11.

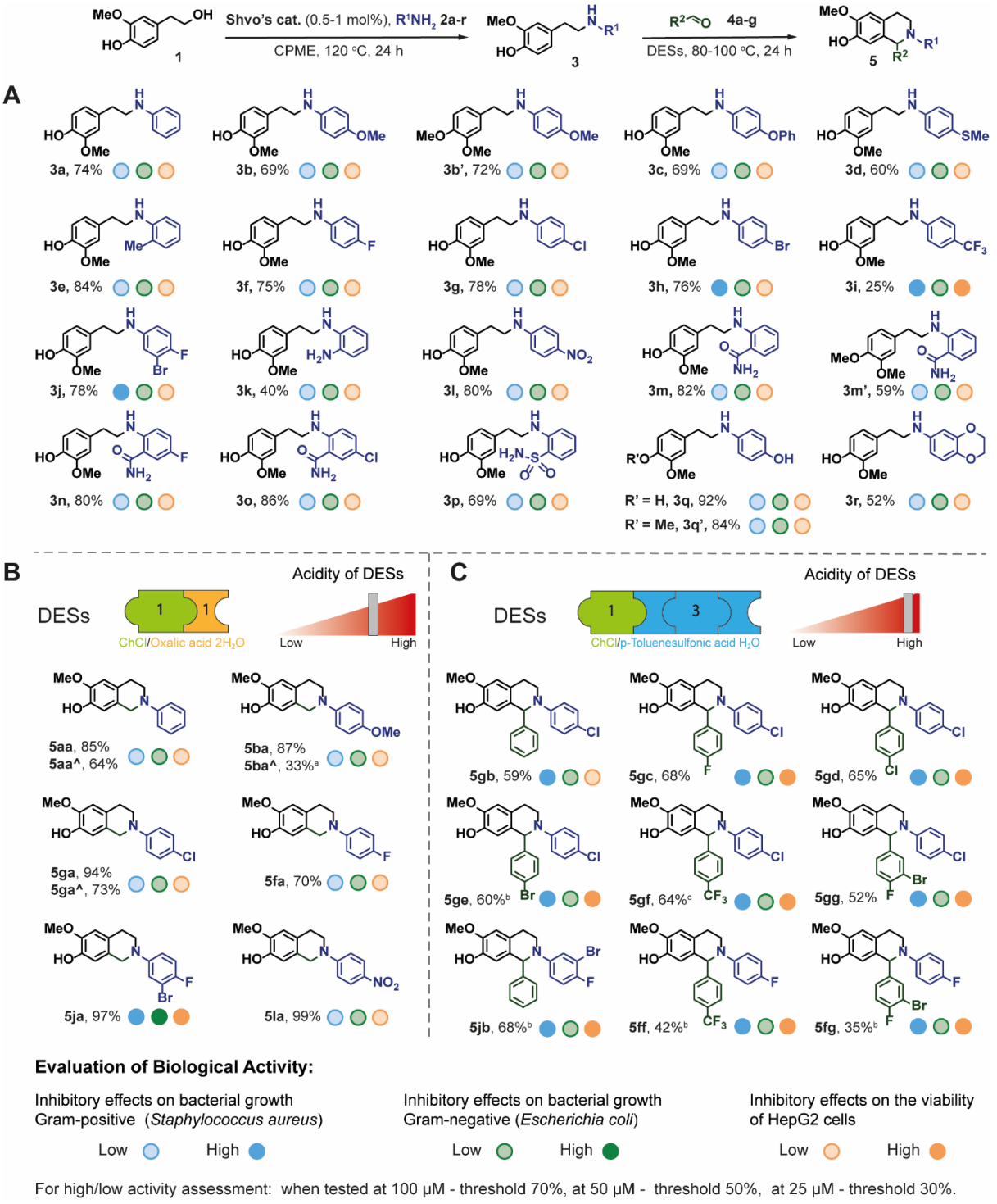

Figure 2. (A) Selective ruthenium-catalyzed amination of homovanillyl alcohol with various amines; (B, C) Construction of lignin-derived tetrahydroisoquinolines (5) in specific deep eutectic solvents. ^ Using HCl-KCl buffer (pH 1, 1 mL, 0.1M)/CPME (1 mL) system instead of DESs. [a] Yield was determined by GC-FID. [b] 1.5 equiv. of corresponding aldehyde was used. [c] 1.5 equiv. of corresponding aldehyde was used, 80 °C.

Construction of tetrahydroisoquinolines in deep eutectic solvents

Next, we aimed to construct variously substituted tetrahydroisoquinolines, privileged moieties in medicinal chemistry (*40*), *via* Pictet–Spengler cyclizations involving the aminoalkyl guaiacols obtained above. To render this step more sustainable, we explored the use of deep eutectic solvents (DESs) instead of commonly applied strong mineral acids (*21*, *41*). Due to their favorable physico-chemical properties (low vapor pressure, potentially non-toxic, biodegradable, and renewable nature), DESs are considered as promising green alternatives for

volatile organic solvents (*42*, *43*). We reasoned that this unique class of alternative reaction media will actively facilitate imine formation and accelerate the subsequent Mannich-type cyclization, both steps involved in the Pictet–Spengler mechanism (*44*). Since these steps are sensitive to the steric and electronic properties of the respective substrates used, as well as the acidity of the reaction medium, we demonstrated that reactivity can be controlled through careful tuning of the DES composition, by selecting appropriate hydrogen bond donors (HBD) and hydrogen-bond acceptors (HBA) (*45*).

High isolated yields of the tetrahydroisoquinolines (**Figure 2B**, **5aa**–**5la**, 70–99%) were achieved by coupling the aminoalkyl-guaiacols (**3a-l**) with paraformaldehyde (**4a**) using natural DESs based on a combination of choline chloride (ChCl) as HBA and oxalic acid dihydrate ($OA{\cdot}2H_2O$) as HBD. Notably, a smooth reaction was seen at 80 ^oC without any strong mineral acid additives, relying solely on the beneficial effect of the DES. As comparison, moderate to good yields (**Figure 2B**, **5aa^**–**5ga^**, 33–73%) were achieved in a hydrochloric acid-potassium chloride buffer (0.1 M, pH 1) (*46*) at higher reaction temperature (120 °C).

However, when the synthesis of 1-substituted tetrahydroisoquinolines was attempted using 4-(2-((4-chlorophenyl)amino)ethyl)-2-methoxyphenol (**3g**) and benzaldehyde (**4b**), the desired cyclization did not occur in $ChCl/OA{\cdot}2H_2O$ even at elevated temperature (120 ^oC) (for more details, see **Table S4**). Taking into account the dependence of the cyclization rate on the acidity of the reaction medium (*47*), we explored DES containing choline chloride (ChCl) as HBA and strong organic acids (*p*-toluenesulfonic acid monohydrate, triflic acid) as HBD component (**Table S4**). The 1-substituted tetrahydroisoquinolines were successfully obtained using the combination of choline chloride and *p*-toluenesulfonic acid monohydrate (ChCl/*p*-TSA in the molar ratio of 1:3) at 100 ^oC, in exceptional selectivity with moderate to good isolated yields (**Figure 2C**).

Sustainable pathways for the synthesis of quinazolin-4(3*H*)-ones and 3-arylindoles

We realized that the substrates **3m-p** offer a unique structural motif that would allow the construction of the quinazolinone moiety, in combination with various carbonyl compounds as coupling partners. And indeed, the reaction of aminoalkyl-phenol **3m** and paraformaldehyde **4a** using hydrochloric acid-potassium chloride buffer, at 100 ^oC (**Figure 3A**) afforded the desired quinazolinone analogue. We assumed that the iminium intermediate, formed upon the coupling of 2-aminobenzamide and the carbonyl compound undergoes a reaction by a nucleophile, such as water, *via* a *6-exo-tet* cyclization followed by the subsequent oxidation of the aminal intermediate (*48*). Remarkably, the target product was delivered in a good 64% isolated yield (**Table S6**, entry 1) on the first attempt. To further improve product selectivity while keeping mild reaction conditions, we were looking to enhance the reactivity by means of a catalyst. Inspired by advances in iridium-catalyzed hydrogen-transfer catalysis (*49*, *50*), we have applied $[Cp^*IrCl_2]_2$ (Cp* = pentamethylcyclopentadienyl) as a catalyst, presuming that it would accelerate the *6-exo-tet* cyclization and in addition facilitate the dehydrogenation of the cyclic aminal formed (*51*). After considerable efforts, we were pleased to find that the desired *N*-heterocycle can be obtained with excellent selectivity (84%) in the presence of only 0.5 mol% of $[Cp^*IrCl_2]_2$ at 100 ^oC in 4 hours (**Table S6**). The scope of the reaction applying a range of 2-aminobenzamides (**3m**–**p**) under the established reaction conditions was examined: the target quinazolinones were delivered in excellent yields (**6ma**–**6pa**, 72–84%) without the need for any additional purification procedure (**Figure 3A**). Interestingly, using glutaraldehyde (**4o**) as a coupling partner, the pharmaceutically-relevant mackinazolinone derivative (*52*) was isolated in 58% yield (**6mo**).

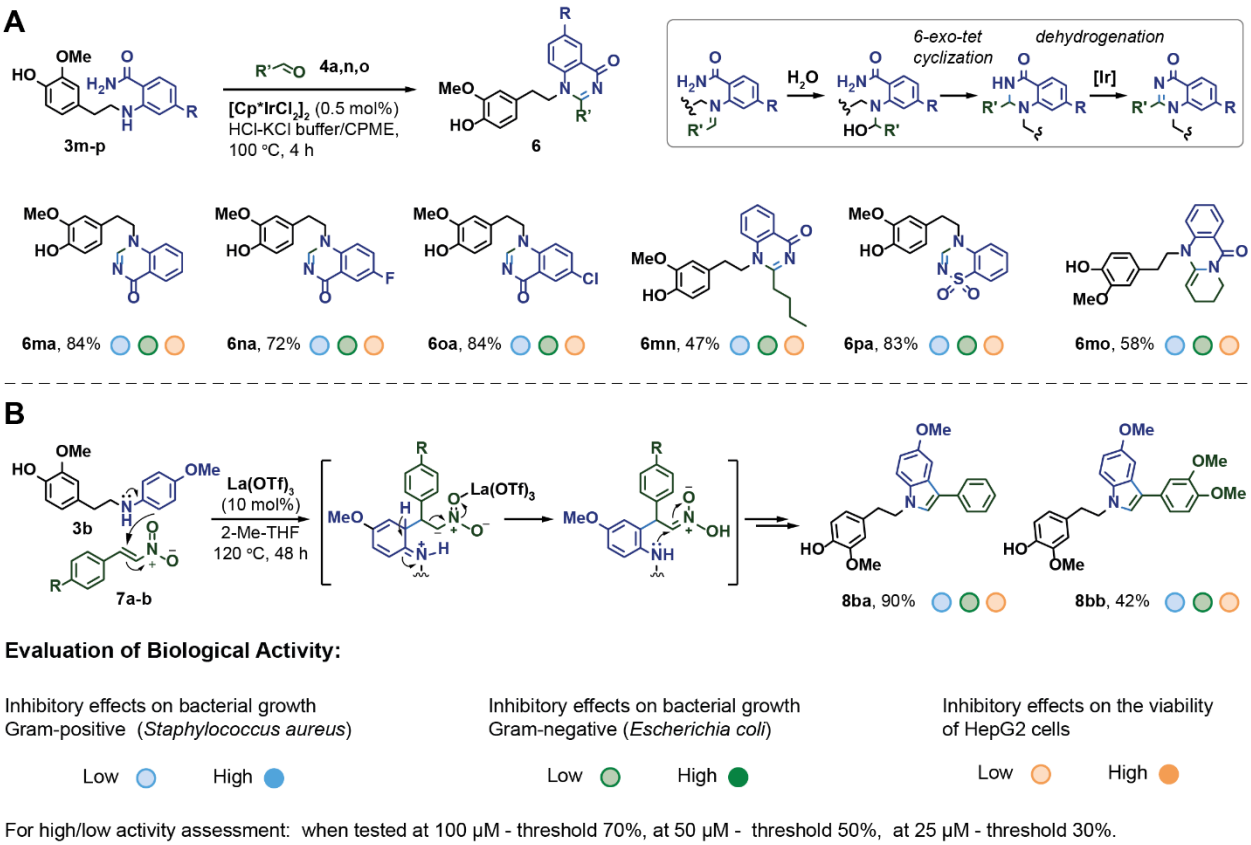

Evaluation of Biological Activity:

Inhibitory effects on bacterial growth Gram-positive (*Staphylococcus aureus*) — Low / High

Inhibitory effects on bacterial growth Gram-negative (*Escherichia coli*) — Low / High

Inhibitory effects on the viability of HepG2 cells — Low / High

For high/low activity assessment: when tested at 100 μM - threshold 70%, at 50 μM - threshold 50%, at 25 μM - threshold 30%.

Figure 3. (A) Synthesis of lignin-derived quinazolin-4(3*H*)-ones and (B) *N*-substituted 3-arylindoles. General reaction conditions **(A)**: **3m-p** (0.2 mmol, 1 equiv.), **4a** (0.22 mmol, 1.1 equiv.), $[Cp^*IrCl_2]_2$ (0.5 mol%, 0.001 mmol), HCl-KCl buffer (pH 1, 1 mL, 0.1M) and CPME (1 mL), 100 °C (temperature of the heating block), 4 h. **(B)**: **3b** (0.15 mmol, 1 equiv.), **7a-b** (0.195 mmol, 1.3 equiv.), $La(OTf)_3$ (10 mol%), 2-Me-THF (2 mL), 120 °C (temperature of the oil bath), 48 h.

Finally, we have constructed *N*-substituted 3-arylindoles through the Lewis acid-catalysed 1,4-addition of *N*-substituted anilines to *trans*-*β*-nitrostyrenes (**Figure 3B**, for more details, see **Table S7**) (*53*). After considerable modification of the reported literature protocol, with focus on the lignin-relevant substrates, we found that 10 mol% of $La(OTf)_3$, and 2-Me-THF as solvent at 120 °C smoothly deliver the desired *N*-aryl 3-arylindole **8ba** in 90% isolated yield. This developed procedure can use renewable vanillin-derived *trans*-*β*-nitrostyrene **7b** and aminoalkyl-phenol **3b**, yielding the target product **8bb** in 42% isolated yield. Considering that *p*-methoxy aniline can also be potentially obtained from lignin (*54*) this approach may serve as a straightforward route to construct the core scaffold of dictyodendrin alkaloids (promising telomerase inhibitors) (*55*), entirely from lignin.

Evaluation of biological activities of the compound libraries

In order to assess the biological activities of the new lignin-based compounds, we followed two approaches, namely cellular activity screening and bioinformatics (**Figure 4**). We screened all compounds of classes **3**, **5**, **6**, and **8** for activities against a representative Gram-positive bacterium (*Staphylococcus aureus*, Newman strain), a Gram-negative bacterium (*Escherichia coli* K12), and a human cancer cell line (HepG2 hepatoma cells).

The aminoalkyl-guaiacols **3** displayed moderate growth inhibitory activities against *S. aureus* and HepG2 cells, whereas they lacked activity against *E. coli* K12 (**Figure 2A** and **Figure S5**). Compounds of the tetrahydroisoquinoline class **5** showed prominent activities against *S. aureus*, HepG2 cells and, interestingly, *E. coli* (**5ja**) (**Figure 2B**, **2C**, and **Figure S5**). On the other hand, compounds of the quinazolinone **6** and indole **8** scaffolds did not show significant

inhibition of bacterial growth, while they displayed moderate cytotoxic activities (**Figure 3A**, **3B**, and **Figure S5**). Accessibility of numerous derivatives of the four classes by virtue of our straightforward synthetic methodology enabled us to study the structure–activity relationships (SARs) indicating the key structural features for activity and establishing the road for further optimization (see Supplementary Information for a detailed discussion).

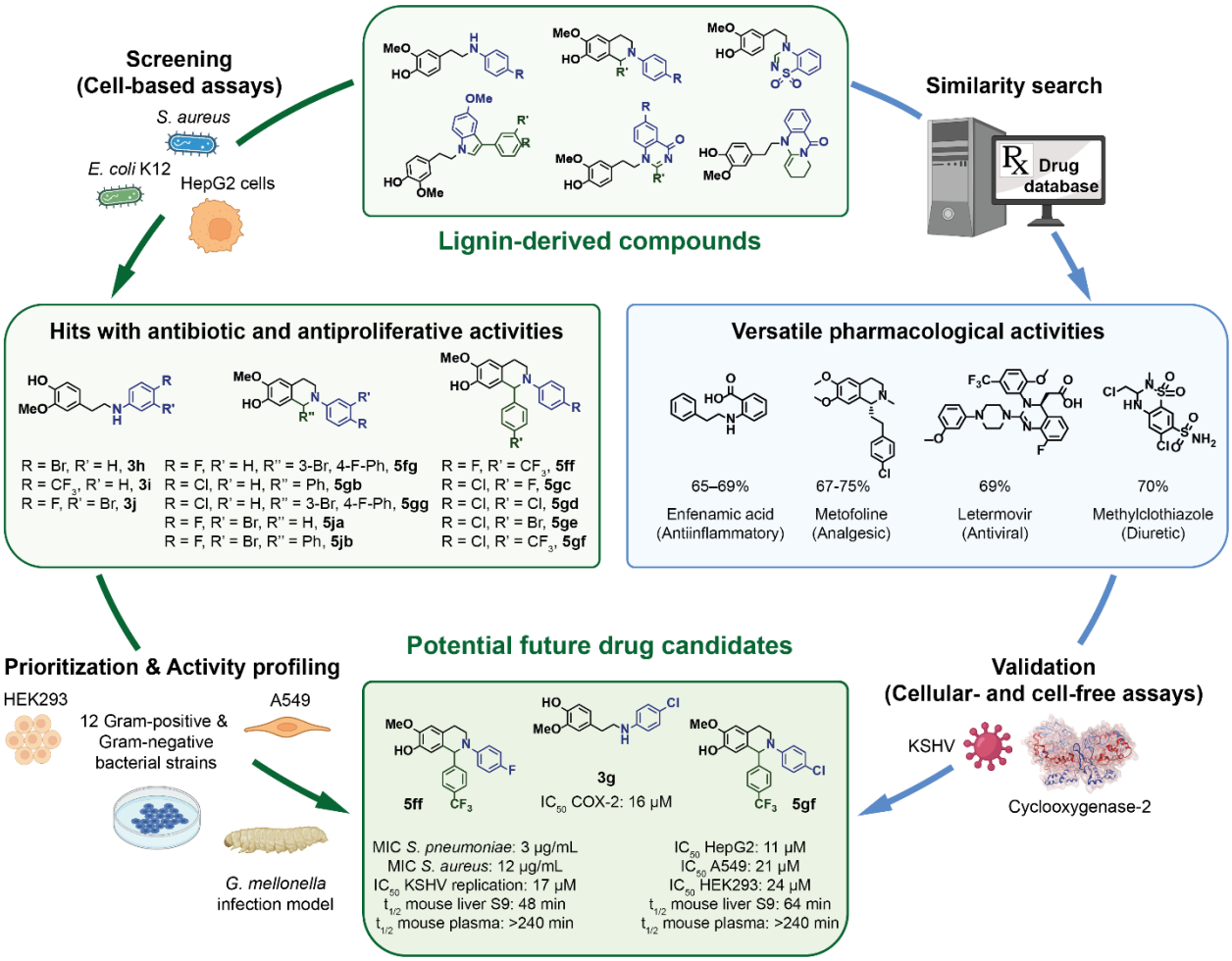

Figure 4. Identification of bioactive lignin-derived molecules through screening and similarity search strategies. Antibacterial and cytotoxicity screening yielded compounds **5ff** and **5gf** with potent activities even in a simple *in vivo* infection model based on *Galleria mellonella* larvae. The similarity assessment revealed structural similarity of the new lignin-based scaffolds to clinically approved drugs for various therapeutic indications. Evaluation of two potential pharmacological activities resulted in compounds **3g** and **5ff** with promising cyclooxygenase-2 inhibition and antiviral activity, respectively.

Next, we determined MIC and IC_{50} values of the most active compounds (**Table S8**). Compound **5ja** shows promising MIC values against both *S. aureus* and *E. coli* of 12.0 ± 4.5 µg/mL and 34.3 ± 1.2 µg/mL, respectively, while compound **5ff** displayed an MIC of 11.8 ± 4.3 µg/mL against *S. aureus*. Regarding the cytotoxic activity, three compounds showed IC_{50} values in HepG2 cells below 25 µM (**5ff**, **5gf**, and **5fg**), where especially **5gf** stood out with an IC_{50} of 11.0 ± 2.0 µM. This strong cytotoxicity encouraged us to investigate **5gf** in two additional human cell lines including lung carcinoma (A549) and human embryonic kidney cells (HEK293). Here, the cytotoxic activity of the compound was confirmed, owing to low IC_{50} values of 21.4 ± 1.1 µM and 24.1 ± 2.3 µM, respectively (**Table S9**).
Furthermore, we tested compounds **5ja** and **5ff** for antibiotic activity against an additional 12 strains including both Gram-positive and Gram-negative pathogens of medical relevance and investigated the role of permeability and efflux for anti-Gram-negative activity (**Table S10**).

Interestingly, the activity of compound **5ja** was improved by about four times, mainly in the *E. coli* mutants Δ*tolc* and Δ*acrB* with defective efflux systems (MIC values between 9 and 10 µg/mL) (**Table S10**). This suggests that **5ja** is a substrate for efflux pumps that deliver the compound back to the outside after penetrating the cell wall. While no activity was observed in the more difficult to penetrate ESKAPE pathogens *Pseudomonas aeruginosa* and *Acinetobacter baumannii*, good MIC values were identified in the Gram-positive strains (8–13 µg/mL) (**Table S10**). The performance of compound **5ff** is particularly noteworthy, which showed no inhibition of Gram-negatives' growth, but inhibited all Gram-positive bacteria. In this context, the antibiotic activity against *Streptococcus pneumoniae* was outstanding, as illustrated by a single-digit MIC value of 2.7 ± 0.1 µg/mL. It is worth mentioning that *S. pneumoniae* is the causative agent of pneumococcal infections and responsible for about 1.6 million deaths every year, according to WHO estimates (*56*). This prompted us to investigate compound **5ff** in a simple and ethically uncritical *in vivo* model based on *G. mellonella* larvae that were infected with *S. pneumoniae* (**Figure S8**). Encouragingly, all three administered doses of compound **5ff** showed a significant and dose-dependent improvement in survival of the animals infected with 10^6 CFU/larva. In particular, the administration of 250 µM resulted in a survival rate of 80%, compared to only 35% in the untreated control (**Figure 5**). This suggests that compound **5ff** is an effective inhibitor of *S. pneumoniae* that can also exert its effect under *in vivo* conditions.

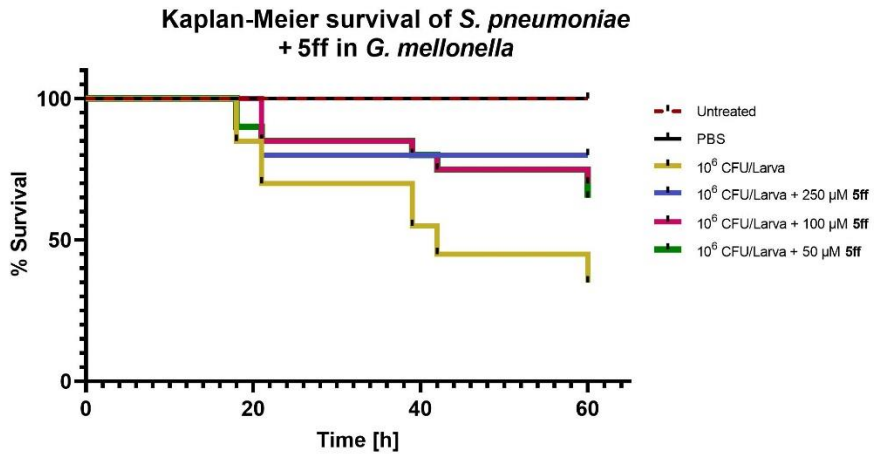

Figure 5. Kaplan-Meier survival analysis of larvae infected with 10^6 CFU/larva of *S. pneumoniae* (strain DSM20566) in combination with several concentrations of compound 5ff. The experiment was conducted over 3 days and each group was monitored twice every day ($p<0.0001$).

Structure similarity approach: design of pharmaceutically active compounds from renewables

In order to identify structurally related pharmaceuticals and potentially additional biological activities of the lignin-based compounds, we carried out chemical similarity analysis (*57*) using a drug database comprising 4,642 approved drugs (**Figure 4**). Representative compounds of scaffolds **3**, **5**, **6**, and **8** were selected as query molecules. To cover a broad chemical space, we utilized two orthogonal fingerprints for similarity assessment, namely BIT_MACCS (atom connectivity) and GpiDAPH3 (pharmacophoric features). Interestingly, the new lignin-derived small molecules displayed marked similarity to several drugs having diverse pharmacological effects such as analgesic, anti-inflammatory, antibiotic, antitumor, antiviral, bronchodilator, diuretic, and neuroprotective activities (**Figure 4** and **Table S13**). For instance, compounds **3o** and **5ga** showed similarity to the cyclooxygenase (COX) inhibitors enfenamic acid and clopirac, whereas compounds **5ff** and **6na** share structural features with letermovir, an antiviral drug against the beta-herpesvirus cytomegalovirus (CMV) (**Table S13**). To verify these predicted activities, first we tested nine selected compounds for COX-2 inhibition. Indeed, all

compounds exhibited significant COX-2 inhibitory activities with compound **3g** showing the highest potency (IC_{50} value of 15.6 ± 2.2 µM) (**Table S11**). Next, we screened compounds **3i**, **5ff** and **6na** for antiviral activity against Kaposi's sarcoma-associated herpesvirus (KSHV), a gamma-herpesvirus. Encouragingly, compounds **3i** and **5ff** displayed a concentration-dependent inhibition of KSHV replication without affecting the viability of HEK293 host cells (**Figure S6**). Moreover, compound **5ff** showed a low micromolar IC_{50} value of 17.4 µM, which is markedly lower than that of the reference antiviral drug foscarnet (IC_{50}: 41.7 µM) (**Figure S7**).

In view of the potential of our frontrunners as novel pharmaceuticals, we determined *in vitro* murine metabolic and plasma stability for compounds **5ff** and **5gf** (see **Figure 4** and **Table S12**). In mouse liver S9 fractions, compound **5ff** demonstrated a significant metabolic stability ($t_{1/2}$ 48 ± 12 min) similar to **5gf** ($t_{1/2}$ 64 ± 17 min). Moreover, both compounds showed excellent plasma stability ($t_{1/2}$ > 240 min). Thus, these compounds represent promising candidates for further optimization and perfectly validates our modular synthetic strategy that is based on rapid modification of bio-based building blocks.

To conclude, in this contribution we adequately demonstrate that the valuable aromatic scaffold of lignin, originating from the amino acids phenylalanine and tyrosine (*11*), represents an excellent basis to the development of sustainable and scalable chemo-catalytic strategies for the synthesis of known natural products as well as various classes of novel biologically active compounds based on the dopamine scaffold. The green catalytic methods introduced allow straightforward access to structurally diverse molecule libraries without the formation of harmful side products and avoiding the use of classical volatile and toxic solvents. This synthesis strategy has enabled the rapid assessment of relevant biological activities relying on *in vitro*, *in vivo* studies and computational similarity searches, with multiple promising hits identified. Compound **5ff** displayed outstanding antibiotic activity against *S. pneumoniae* - the causative agent of pneumococcal infections and an important priority pathogen according to WHO. Compound **5gf** showed anti-proliferative activity on three cell lines in the low micromolar range. Computer-aided structural similarity search compared the new lignin-based scaffolds to clinically approved drugs and resulted in identifying compounds **3g** and **5ff** with promising cyclooxygenase-2 inhibition and antiviral activity against KSHV, indicating future promising therapeutic application areas with unmet medical needs (*58*). Compounds **5ff** and **5gf** of the tetrahydroisoquinoline class exhibited remarkable metabolic and plasma stabilities, opening the door for further pharmaceutical development.

By providing creative strategies for the construction of relevant biologically active scaffolds from biomass depolymerization products, guided by cellular activity and chemical similarity search methods, this contribution provides a clear way forward for the integration of green manufacturing practices in the discovery of novel therapeutic agents, at the same time enabling the defossilization of the pharmaceutical industry. With lignocellulosic biorefineries gaining increasing importance in efforts to reduce our dependence on petroleum (*59*), this strategy opens new possibities towards high-end and high-value target molecules, which are essential to increase the overall economic fesasibility of such biorefineries.

References and Notes

1. Active Pharmaceutical Ingredients Market Report, 2021–2028, Grand View Research, https://www.grandviewresearch.com/industry-analysis/active-pharmaceutical-ingredientsmarket.
2. J. Park, M. A. Kelly, J. X. Kang, S. S. Seemakurti, J. L. Ramirez, M. C. Hatzell, C. Sievers, A. S. Bommarius, Production of active pharmaceutical ingredients (APIs) from lignin-derived phenol and catechol. *Green Chem.* **23**, 7488–7498 (2021).
3. R. A. Sheldon, The: E factor 25 years on: The rise of green chemistry and

sustainability. *Green Chem.* **19**, 18–43 (2017).

4. L. Wollensack, K. Budzinski, J. Backmann, Defossilization of pharmaceutical manufacturing. *Curr. Opin. Green Sustain. Chem.* **33**, 100586 (2022).

5. H. Sneddon, Embedding sustainable practices into pharmaceutical R&D: what are the challenges? *Futur. Med. Chem.* **6**, 1373–1376 (2014).

6. M. C. Bryan, P. J. Dunn, D. Entwistle, F. Gallou, S. G. Koenig, J. D. Hayler, M. R. Hickey, S. Hughes, M. E. Kopach, G. Moine, P. Richardson, F. Roschangar, A. Steven, F. J. Weiberth, Key Green Chemistry research areas from a pharmaceutical manufacturers' perspective revisited. *Green Chem.* **20**, 5082–5103 (2018).

7. United Nations, Department of Economic and Social Affairs, Sustainable Development, National strategies and SDG integration, https://sdgs.un.org/topics/national-sustainable-de.

8. S. Elangovan, A. Afanasenko, J. Haupenthal, Z. Sun, Y. Liu, A. K. H. Hirsch, K. Barta, From Wood to Tetrahydro-2-benzazepines in Three Waste-Free Steps: Modular Synthesis of Biologically Active Lignin-Derived Scaffolds. *ACS Cent. Sci.* **5**, 1707–1716 (2019).

9. Z. Sun, G. Bottari, A. Afanasenko, M. C. A. Stuart, P. J. Deuss, B. Fridrich, K. Barta, *Nat. Catal.*, **1**, 82–92 (2018).

10. A. Afanasenko, K. Barta, Pharmaceutically relevant (hetero)cyclic compounds and natural products from lignin-derived monomers: Present and perspectives. *iScience*. **24**, 102211 (2021).

11. W. Boerjan, J. Ralph, M. Baucher, Lignin Biosynthesis. *Annu. Rev. Plant Biol.* **54**, 519–546 (2003).

12. X. Ma, S. Huang, M. Li, R. Luque, N. Yan, Catalytic conversion of low carbon and sustainable resources. *Catal. Today*. **368**, 1–290 (2021).

13. A. Rahimi, A. Ulbrich, J. J. Coon, S. S. Stahl, Formic-acid-induced depolymerization of oxidized lignin to aromatics. *Nature*. **515**, 249–252 (2014).

14. A. J. Ragauskas, G. T. Beckham, M. J. Biddy, R. Chandra, F. Chen, M. F. Davis, B. H. Davison, R. A. Dixon, P. Gilna, M. Keller, P. Langan, A. K. Naskar, J. N. Saddler, T. J. Tschaplinski, G. A. Tuskan, C. E. Wyman, Lignin valorization: Improving lignin processing in the biorefinery. *Science.* **344**, 1246843 (2014).

15. C. O. Tuck, E. Pérez, I. T. Horváth, R. A. Sheldon, M. Poliakoff, Valorization of biomass: Deriving more value from waste. *Science.* **337**, 695 (2012).

16. X. Chen, S. Song, H. Li, G. Gözaydln, N. Yan, Expanding the Boundary of Biorefinery: Organonitrogen Chemicals from Biomass. *Acc. Chem. Res.* **54**, 1711–1722 (2021).

17. Z. Mycroft, M. Gomis, P. Mines, P. Law, T. D. H. Bugg, Biocatalytic conversion of lignin to aromatic dicarboxylic acids in Rhodococcus jostii RHA1 by re-routing aromatic degradation pathways. *Green Chem.* **17**, 4974–4979 (2015).

18. J. Ralph, S. Karlen, J. Mobley, Synthesis of Paracetamol (Acetaminophen) from biomass-derived P-hydroxybenzamide (2019), US 10286504 B2.

19. S. Bähn, S. Imm, L. Neubert, M. Zhang, H. Neumann, M. Beller, The catalytic amination of alcohols. *ChemCatChem*. **3**, 1853–1864 (2011).

20. S. Elangovan, J. Neumann, J. B. Sortais, K. Junge, C. Darcel, M. Beller, Efficient and

selective N-alkylation of amines with alcohols catalysed by manganese pincer complexes. *Nat. Commun.* **7**, 12641 (2016).

21. E. L. Smith, A. P. Abbott, K. S. Ryder, Deep Eutectic Solvents (DESs) and Their Applications. *Chem. Rev.* **114**, 11060–11082 (2014).
22. P. J. Deuss, M. Scott, F. Tran, N. J. Westwood, J. G. De Vries, K. Barta, Aromatic Monomers by in Situ Conversion of Reactive Intermediates in the Acid-Catalyzed Depolymerization of Lignin. *J. Am. Chem. Soc.* **137**, 7456–7467 (2015).
23. P. J. Deuss, C. W. Lahive, C. S. Lancefield, N. J. Westwood, P. C. J. Kamer, K. Barta, J. G. de Vries, Metal Triflates for the Production of Aromatics from Lignin. *ChemSusChem*. **9**, 2974–2981 (2016).
24. A. De Santi, M. V. Galkin, C. W. Lahive, P. J. Deuss, K. Barta, Lignin-First Fractionation of Softwood Lignocellulose Using a Mild Dimethyl Carbonate and Ethylene Glycol Organosolv Process. *ChemSusChem*. **13**, 4468–4477 (2020).
25. M. V. Galkin, J. S. M. Samec, Lignin Valorization through Catalytic Lignocellulose Fractionation: A Fundamental Platform for the Future Biorefinery. *ChemSusChem*. **9**, 1544–1558 (2016).
26. Y. M. Questell-Santiago, M. V. Galkin, K. Barta, J. S. Luterbacher, Stabilization strategies in biomass depolymerization using chemical functionalization. *Nat. Rev. Chem.* **4**, 311–330 (2020).
27. A. De Santi, S. Monti, G. Barcaro, Z. Zhang, K. Barta, P. J. Deuss, New Mechanistic Insights into the Lignin β-O-4 Linkage Acidolysis with Ethylene Glycol Stabilization Aided by Multilevel Computational Chemistry. *ACS Sustain. Chem. Eng.* **9**, 2388–2399 (2021).
28. K. W. Bentley, β-Phenylethylamines and the isoquinoline alkaloids. *Nat. Prod. Rep.* **23**, 444–463 (2006).
29. J. D. Scott, R. M. Williams, Chemistry and biology of the tetrahydroisoquinoline antitumor antibiotics. *Chem. Rev.* **102**, 1669–1730 (2002).
30. M. Iranshahy, R. J. Quinn, M. Iranshahi, Biologically active isoquinoline alkaloids with drug-like properties from the genus Corydalis. *RSC Adv.* **4**, 15900–15913 (2014).
31. J. M. Hagel, P. J. Facchini, Benzylisoquinoline alkaloid metabolism: A century of discovery and a brave new world. *Plant Cell Physiol.* **54**, 647–672 (2013).
32. G. A. W. Beaudoin, P. J. Facchini, Benzylisoquinoline alkaloid biosynthesis in opium poppy. *Planta*. **240**, 19–32 (2014).
33. P. J. Deuss, C. S. Lancefield, A. Narani, J. G. De Vries, N. J. Westwood, K. Barta, Phenolic acetals from lignins of varying compositions: Via iron(iii) triflate catalysed depolymerisation. *Green Chem.* **19**, 2774–2782 (2017).
34. A. C. Whitfield, B. T. Moore, R. N. Daniels, Classics in chemical neuroscience: Levodopa. *ACS Chem. Neurosci.* **5**, 1192–1197 (2014).
35. H. Knust, M. Nettekoven, E. Pinard, O. Roche, M. Rogers-Evans, Monoamide derivatives as orexin receptor antagonists (2009), WO 2009/016087 A1.
36. A. M. Kanhed, A. Sinha, J. Machhi, A. Tripathi, Z. S. Parikh, P. P. Pillai, R. Giridhar, M. R. Yadav, Discovery of isoalloxazine derivatives as a new class of potential anti-Alzheimer agents and their synthesis. *Bioorg. Chem.* **61**, 7–12 (2015).
37. J. Liang, J. Chen, J. Liu, L. Li, H. Zhang, Oxidative dearomatization in the synthesis of

erythrina, oxindole and hexahydropyrrolo[2,3-b]indole skeletons. *Chem. Commun.* **46**, 3666–3668 (2010).

38. Z. Q. Pan, J. X. Liang, J. B. Chen, X. D. Yang, H. Bin Zhang, Oxidative dearomatic approach towards the synthesis of erythrina skeleton: a formal synthesis of demethoxyerythratidinone. *Nat. Products Bioprospect.* **1**, 129–133 (2011).

39. S. Curia, A. Biundo, I. Fischer, V. Braunschmid, G. M. Gübitz, J. F. Stanzione, Towards Sustainable High-Performance Thermoplastics: Synthesis, Characterization, and Enzymatic Hydrolysis of Bisguaiacol-Based Polyesters. *ChemSusChem*. **11**, 2529–2539 (2018).

40. I. Khan, A. Ibrar, W. Ahmed, A. Saeed, Synthetic approaches, functionalization and therapeutic potential of quinazoline and quinazolinone skeletons: The advances continue. *Eur. J. Med. Chem.* **90**, 124–169 (2015).

41. S. Handy, M. Wright, An acid-free Pictet-Spengler reaction using deep eutectic solvents (DES). *Tetrahedron Lett.* **55**, 3440–3442 (2014).

42. F. Jérôme, R. Luque, *Bio-Based Solvents* (John Wiley & Sons, 2017).

43. Q. Zhang, K. De Oliveira Vigier, S. Royer, F. Jérôme, Deep eutectic solvents: Syntheses, properties and applications. *Chem. Soc. Rev.* **41**, 7108–7146 (2012).

44. J. Stöckigt, A. P. Antonchick, F. Wu, H. Waldmann, The pictet-spengler reaction in nature and in organic chemistry. *Angew. Chem. Int. Ed.* **50**, 8538–8564 (2011).

45. Y. Liu, N. Deak, Z. Wang, H. Yu, L. Hameleers, E. Jurak, P. J. Deuss, K. Barta, Tunable and functional deep eutectic solvents for lignocellulose valorization. *Nat. Commun.* **12**, 5424 (2021).

46. T. Pesnot, M. C. Gershater, J. M. Ward, H. C. Hailes, Phosphate mediated biomimetic synthesis of tetrahydroisoquinoline alkaloids. *Chem. Commun.* **47**, 3242–3244 (2011).

47. A. Yokoyama, T. Ohwada, K. Shudo, Prototype Pictet-Spengler reactions catalyzed by superacids. Involvement of dicationic superelectrophiles. *J. Org. Chem.* **64**, 611–617 (1999).

48. N. Y. Kim, C. H. Cheon, Synthesis of quinazolinones from anthranilamides and aldehydes via metal-free aerobic oxidation in DMSO. *Tetrahedron Lett.* **55**, 2340–2344 (2014).

49. D. Wang, D. Astruc, The Golden Age of Transfer Hydrogenation. *Chem. Rev.* **115**, 6621–6686 (2015).

50. A. Bartoszewicz, N. Ahlsten, B. Martín-Matute, Enantioselective synthesis of alcohols and amines by iridium-catalyzed hydrogenation, transfer hydrogenation, and related processes. *Chem. - A Eur. J.* **19**, 7274–7302 (2013).

51. J. Zhou, J. Fang, One-pot synthesis of quinazolinones via iridium-catalyzed hydrogen transfers. *J. Org. Chem.* **76**, 7730–7736 (2011).

52. A. O. Nasrullaev, Z. E. Turdibaev, B. Z. Elmuradov, A. Yili, H. A. Aisa, K. M. Shakhidoyatov, Chemical transformations of mackinazolinone and its derivativesa. *Chem. Nat. Compd.* **48**, 638–642 (2012).

53. R. Gattu, S. Bhattacharjee, K. Mahato, A. T. Khan, Electronic effect of substituents on anilines favors 1,4-addition to: Trans -β-nitrostyrenes: Access to N -substituted 3-arylindoles and 3-arylindoles. *Org. Biomol. Chem.* **16**, 3760–3770 (2018).

54. E. Blondiaux, J. Bomon, M. Smoleń, N. Kaval, F. Lemière, S. Sergeyev, L. Diels, B.

Sels, B. U. W. Maes, Bio-based Aromatic Amines from Lignin-Derived Monomers. *ACS Sustain. Chem. Eng.* **7**, 6906–6916 (2019).

55. W. Zhang, J. M. Ready, Total synthesis of the dictyodendrins as an arena to highlight emerging synthetic technologies. *Nat. Prod. Rep.* **34**, 1010–1034 (2017).

56. Pneumococcal conjugate vaccines. WHO, retrieved on the 15th of March 2022; https://www.who.int/teams/health-product-policy-and-standards/standards-and-specifications/vaccines-quality/pneumococcal-conjugate-vaccines.

57. G. Maggiora, M. Vogt, D. Stumpfe, J. Bajorath, Molecular similarity in medicinal chemistry. *J. Med. Chem.* **57**, 3186–3204 (2014).

58. E. Naimo, J. Zischke, T. F. Schulz, Recent advances in developing treatments of kaposi's sarcoma herpesvirus-related diseases. *Viruses*. **13**, 1797 (2021).

59. W. Lan, J. S. Luterbacher, A Road to Profitability from Lignin via the Production of Bioactive Molecules. *ACS Cent. Sci.* **5**, 1642–1644 (2019).

Acknowledgments: The authors thank J. Jung, T. Wittmann and S. Wolter for excellent technical support. Illustrations of cells, bacteria, etc. were created with BioRender.com.

Funding: ERC starting grant 757913 and Helmholtz Association's Initiative and Networking Fund (AKHH). K. B. is grateful for financial support from the European Research Council, ERC Starting Grant 2015 (CatASus) 638076 and ERC Proof of Concept Grant 2019 (PURE) 875649. This work is part of the research program Talent Scheme (Vidi) with project number 723.015.005, which is partly financed by The Netherlands Organization for Scientific Research (NWO). X. W. is grateful for financial support from the China Scholarship Council (grant number 201808330391).

Author contributions:

Conceptualization: AMA, AKHH, KB

Methodology: AMA, XW, ADS, WAME, AMK, RS, MSS, TS, JH, AKHH, KB

Investigation: AMA, XW, ADS, WAME, AMK, RS, MSS, TS, JH, AKHH, KB

Visualization: AMA

Funding acquisition: AKHH, KB

Project administration: AKHH, KB

Supervision: AKHH, KB

Writing – original draft: AMA, KB

Writing – review & editing: AMA, XW, ADS, WAME, AMK, RS, MSS, TS, JH, AKHH, KB

Competing interests: Authors declare that they have no competing interests.

Data and materials availability: All data are available in the main text or the supplementary materials.